The role of interfacial lattice Ag$^+$ on titania based photocatalysis

Hongyun Yang, Feng Chen*, Yanchao Jiao, Jinlong Zhang

Key Laboratory for Advanced Materials and Institute of Fine Chemicals, East China University of Science and Technology, 130 Meilong Road, Shanghai 200237, PR China

ABSTRACT

Ag^0/Ag$^+$/TiO$_2$ composites were prepared via alkalescent hydrothermal process in aqueous ammonia, and Ag$^+$/TiO$_2$ was prepared by eluting the Ag^0 cluster from the Ag^0/Ag$^+$/TiO$_2$ composites with K$_3$[Fe(CN)$_6$]/aqueous ammonia. Methyl orange (MO) and Rhodamine B (RhB) were used to test the photocatalytic activity of the photocatalysts. The photocatalytic activity of the composites was greatly improved after eluting Ag^0 clusters from the Ag^0/Ag$^+$/TiO$_2$ composites. Interfacial lattice Ag$^+$ cations but not Ag^0 clusters are responsible for improving the photocatalytic performance of the composites in this work. XPS measurement shows that the chemical state of the interfacial lattice Ag$^+$ cation is different with the surface chemical adsorbed Ag$^+$ cation. Surface chemical adsorbed Ag$^+$ cation is invalid to promote the photocatalytic activity of TiO$_2$ while Na$^+$ cation can cancel the promotional effect of the interfacial lattice Ag$^+$ cation by competitively occupying the interfacial lattice defects. The 2 h turn over numbers of the interfacial lattice Ag$^+$ cations to the degradation of MO and RhB reach 8 and 10, respectively, which show that the interfacial lattice Ag$^+$ cations act as recyclable catalytic sites but not one-time consumptive species.

© 2012 Elsevier B.V. All rights reserved.

1. Introduction

Titania has been frequently concerned in photocatalysis for environmental applications and solar energy conversion [1,2]. Generally, the absorption of UV photons leads to the electron transition in TiO$_2$. Then, the photogenerated electrons and holes transfer to the interface of TiO$_2$ and go on the interfacial redox processes which produce active species. It has been confirmed that various modifications on the interface of titania can promote the interfacial redox processes by enhancing separation of the photogenerated electrons and holes, such as noble metal loading [3,4], binary (semiconductor) compositing [5–8].

Generally, Schottky barrier mechanism is used to understand the promotion role of noble metal cluster loaded on TiO$_2$. The barrier forms at the interface of metal/titania works as an electron trap and thus restrains the recombination of charge carriers during the photocatalytic processes. The photocatalytic performance of noble metal loaded titania relies heavily on the quantum size effect of the noble metal cluster [9]. For instance, the titania loaded with 1.87 nm diameter gold nanoparticles was reported to have the best photocatalytic activity for water splitting [10].

However, when researchers shift their focus on the visible light photocatalysis of noble metal cluster loaded titania for better solar utilization, an inverse electron transfer mechanism begins to appear. Surface plasmon resonance (SPR) of noble metal clusters such as Au^0 and Ag^0 is suggested to play the key role for visible light absorption and endow the catalyst a visible light photocatalytic activity [11,12]. The photoexcited electrons produced via the enhanced near-field amplitude are transferred into the conduction band (CB) of titania, and subsequently conduct reaction with the adsorbed O$_2$ at the interface of titania. One may notice that a back electron transfer from CB of titania to metal cluster (i.e. Schottky barrier mechanism) would definitely result in a cancelation for the visible photocatalytic activity of noble metal cluster crystals loaded titania.

The work reported here focuses on raising the concerns about the chemical nature of interfacial interaction between the noble metal species and titania in the photocatalytic process, which has not yet been paid close attention. Literatures [13,14] have reported that the practical photocatalytic performance of the noble metal cluster loaded titania depends strongly on the preparation method, the nature of titania and even the thermal treatment procedure of the catalyst. Besides the lattice phase and the size of titania nanoparticle as well as the size of the metal cluster, all the above factors would unavoidably vary the interface characteristics of the noble metal cluster loaded titania, where noble metal ions probably occupy a number of interfacial lattice vacancies. Interestingly, a previous work [15] on the thermal catalytic oxidative activity of Au clusters loaded ceria displayed that the catalytic activity was almost unaffected by the removal of Au^0 metallic clusters for the oxidation of CO. The gold cations trapped in surface defects of ceria,

that is the ionic gold, was suggested to strongly interact with the ceria support and be the active site for the reaction.

In this work, the Ag clusters loaded titania was prepared via an alkalescent hydrothermal process, in which Ag^+ cations initially intercalate into the interlayer of ammonium titanate via ion-exchange and then are gradually ejected during the hydrothermal phase transition from titanate into anatase. In this way, Ag^+ cations are expected to occupy more interfacial lattice defects than the normal impregnation methods, although most of Ag^+ cations were reduced and formed Ag^0 clusters on the surface of TiO_2. The as-prepared Ag^0 clusters loaded titania is thus labeled as $Ag^0/Ag^+/TiO_2$ which contains a number of O^{2-}—Ag^+—O^{2-} bond connections at the interfacial lattice defects of titania.

2. Experimental

2.1. Reagents and materials

Tetrabutyl titanate (TBT) and $NH_3 \cdot H_2O$ (25–28%) were obtained from Ling Feng Chemical Reagent. $AgNO_3$, $NaNO_3$, and $K_3[Fe(CN)_6]$ were obtained from Sinopharm Chemical Reagent. Methyl orange (MO) and Rhodamine B (RhB) were obtained from Acros. All the reagents were of AR and used as received. Doubly distilled water was used throughout the work.

2.2. Catalyst preparation

2.2.1. Preparation of Ag-loaded TiO2

The preparation of Ag^0-loaded TiO_2 was carried out according to the alkalescent hydrothermal procedures reported in our previous works [16]. A certain amount of $AgNO_3$ (Ag/Ti molar ratio of 0, 1%, 2%, 3%, 4% and 5%, respectively) was dissolved into aqueous ammonia ($NH_3 \cdot H_2O$). Then 7.8 ml TBT was directly hydrolyzed in the above solution. The total volume of solution was controlled to 75 ml. After stirring for a short time the resulting suspension was transferred to a Teflon-lined autoclave and heated to 180 °C for 24 h. The residual Ag^+ in the filtrate was detected with KI aqueous solution. The results showed that all the Ag^+ ions in the system were embedded into the catalyst and dissolved Ag^+ was below the detection limit. The obtained Ag-loaded TiO_2 powders were then washed with water and dried at 80 °C for 24 h.

In order to reveal the interference of other cations, Ag-loaded TiO_2 was also prepared in the presence of Na^+. In this case, the hydrolysis and the hydrothermal process were carried out in the presence of both Na^+ and Ag^+ with total cation (Na^+ and Ag^+) concentration of 0.125 M and 0.25 M, respectively. Our previous works [17–19] show Na^+ ion plays a crucial role in the phase transition process from titanate into titania. Generally, Na^+ ion has stronger electrostatic interaction with the minus charged titanate host layers, and thus Na^+ ion would prefer to intercalate into the interlayer of the titanate by ion-exchanging. As Na^+ ion has competitive advantage in intercalating into the interlayer of titanate and occupying the interfacial lattice defect sites of TiO_2 to the Ag^+ ion, the presence of Na^+ ion should be adverse to form interfacial lattice Ag^+ ion during the hydrothermal preparation of Ag-loaded TiO_2. Therefore, changes on the effect of interfacial lattice Ag^+ is expected to be observed in the Ag-loaded TiO_2 composites prepared in the presence of Na^+.

2.2.2. Preparation of Ag0-free TiO2 from Ag-loaded TiO2

The Ag^0 free Ag^+/TiO_2 with an unaltered titania physicochemical properties was prepared by leaching of the surface loaded Ag^0 cluster with $K_3[Fe(CN)_6]$/aqueous ammonia solution [16]. $K_3[Fe(CN)_6]$ of 0.1 g was dissolved into 50 ml water. As-prepared Ag^0-loaded TiO_2 catalyst of 0.5 g was dispersed into 50 ml water under stirring. Then the as-prepared $K_3[Fe(CN)_6]$ solution was added into

the catalyst suspension. After an interval of 30 min, 1.5 ml aqueous ammonia was added into the suspension under stirring. After stirring for ca. 1.5 h, the suspension was then filtered and carefully washed with water to obtain the final Ag^0-free powder and dried at 80 °C for 24 h.

2.3. Catalyst characterization

Catalyst samples were characterized by powder X-ray diffraction (XRD), transmission electron microscopy (TEM), high-resolution transmission electron microscopy (HRTEM), Brunauer–Emmett–Teller (BET) method, X-ray photoelectron spectroscopy (XPS) and cyclic voltammetry (CV).

The crystallographic information of products in this paper was examined by powder XRD diffraction patterns of these samples were performed using a powder diffractometer (RIGAKU D/max2550) operating in the reflection mode with a Siemens D5000 diffractometer (Cu Kα) at a scan rate of 0.02° 2θ s^{-1}. Both TEM and HRTEM were investigated using a JEOL JEM 2100F instrument operated at 200 kV and equipped with an EDX facility as well as with the potential of performing SAED. To prepare the HRTEM specimens, the powder samples were first dispersed ultrasonically in absolute ethanol. One drop of the suspension was placed on a carbon film supported on a copper grid and allowed to dry in air before the specimens were transferred into the microscope. The instrument employed for XPS studies was a Perkin-Elmer PHI 5000C ESCA system with Mg Kα radiation (photon energy 1253.6 eV) operated at 300 W, and calibrated internally by carbon deposit C (1s) binding energy (BE) at 284.6 eV. The BET surface area was determined with a Micromeritics' ASAP 2020M equipment. Disposable screen printed carbon electrode (SPCE) with three-electrode system was fabricated for CV measurement. The CV measurements were performed at CHI 660 electrochemical workstation in 0.4 M KNO_3 solutions, which were degassed with nitrogen for 15 min.

2.4. Photocatalytic activity test

The catalytic activity under UV light was investigated by the photodegradation of MO and RhB. UV irradiation was carried out using a 300 W high-pressure mercury lamp, which was surrounded by a quartz jacket to allow for water cooling. Typically, photocatalyst powder (0.10 g) was added into 100 ml 10 mg L^{-1} aqueous MO solution (or 20 mg L^{-1} RhB solution) and magnetically stirred in the dark for 30 min before UV illumination was conducted. The absorbance of MO at 465 nm (553 nm in the case of RhB) was monitored by measuring with a UV–vis spectrophotometer (Shimadzu UV-2450).

3. Results and discussion

3.1. Crystal phase and morphology of catalysts

Fig. 1 presents the XRD patterns of the Ag-loaded TiO_2 photocatalyst samples prepared with various dosages of Ag^+. The XRD patterns show that titania in the as-prepared catalysts is in the form of anatase (JCPDS No. 71-1167), and Ag^0 cluster (cubic, JCPDS No. 65-2871) has also formed for the catalysts prepared in the presence of Ag^+. The amount of Ag^0 clusters increases with the increase of the $AgNO_3$/TBT molar ratio in the hydrothermal preparation of $Ag^0/Ag^+/TiO_2$ composites, while the crystal phase and the grain size of TiO_2 seem unchanged.

Fig. 2 presents the XRD patterns of the Ag-loaded TiO_2 photocatalyst samples after the $K_3[Fe(CN)_6]$/aqueous ammonia elution treatment. After the treatment of $K_3[Fe(CN)_6]$/aqueous ammonia, the XRD signals ascribed to Ag^0 clusters disappear, which confirms Ag^0 clusters on the surface of anatase titania were washed
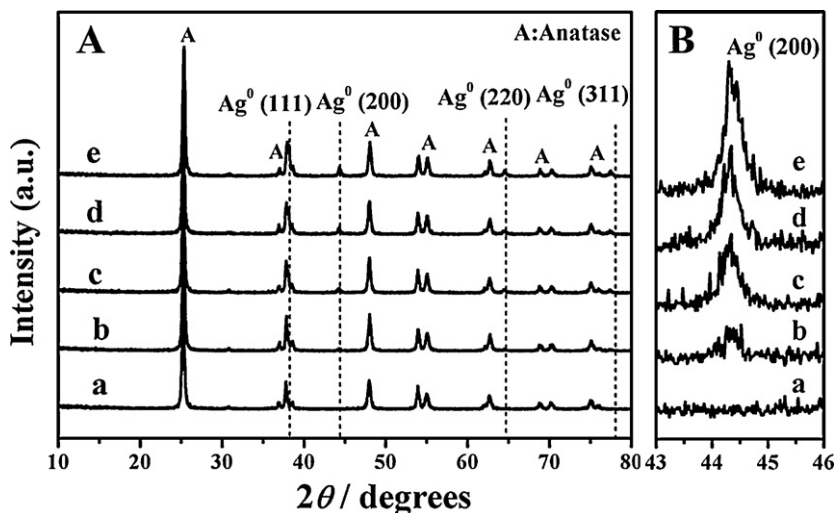
Fig. 1. (A) XRD patterns of the (a) 0.0%, (b) 1%, (c) 2%, (d) 3%, and (e) 4% Ag-loaded TiO$_2$. (B) Ag^0 (2 0 0) peaks in magnification.

away. The crystal phase, crystallinity and the grain size of TiO$_2$ are unchanged before and after K$_3$[Fe(CN)$_6$]/aqueous ammonia elution.

Generally, TBT would rapidly form amorphous ammonium titanate when it was mixed with aqueous ammonia. When cation such as Ag$^+$ was presented in the aqueous ammonia, it would initially intercalate into the interlayer of ammonium titanate via ion-exchange. During the hydrothermal process, titanate hydrothermally phase transit into anatase, accompanied with a gradually ejection of Ag$^+$ cation as the size of Ag$^+$ cation is much larger than that of Ti^{4+}. However, although most of Ag$^+$ cations were reduced and formed Ag^0 clusters on the surface of TiO$_2$ as we observed, Ag$^+$ cations are expected to occupy more interfacial lattice defects than the normal impregnation methods in this way. Thus, the as-prepared Ag^0 clusters loaded titania is labeled as Ag^0/Ag$^+$/TiO$_2$ hereinafter which contains a number of O^{2-}—Ag$^+$—O^{2-} bond connections at the interfacial lattice defects of titania.

During the K$_3$[Fe(CN)$_6$]/aqueous ammonia elution, the Ag^0 atoms were entirely oxidized to [Ag(NH$_3$)$_2$]$^+$ with K$_3$[Fe(CN)$_6$] and thus dissolved to the solvent. Meanwhile, the bonded Ag$^+$ cations at the interfacial lattice defects sites of titania were left unchanged. Accordingly, the Ag-loaded TiO$_2$ after the K$_3$[Fe(CN)$_6$]/aqueous ammonia elution was labeled as Ag$^+$/TiO$_2$ hereinafter. For comparison purposes, the surface chemically adsorbed Ag$^+$ content of

Ag$^+$/TiO$_2$ (designated as P-Ag$^+$/TiO$_2$) was also prepared with a post-adsorption process in a AgNO$_3$ solution.

HRTEM images in Fig. 3 show the anatase titania has a spindly morphology. Ag^0 clusters have a uniform diameter of less than 2.0 nm homogeneously disperse on the surface of TiO$_2$ crystallites in 2.0% Ag^0/Ag$^+$/TiO$_2$ (Ag/Ti = 2.0 atm%) (Fig. 3a–c), which however cannot be observed after the K$_3$[Fe(CN)$_6$]/aqueous ammonia eluting(Fig. 3d). In short, Ag^0/Ag$^+$/TiO$_2$ and Ag$^+$/TiO$_2$ were prepared artfully with just similar TiO$_2$ host. The properties of the thus-prepared Ag^0/Ag$^+$/TiO$_2$ and Ag$^+$/TiO$_2$ samples are presented in Table 1. It is found that the crystallite size and the specific surface area changes little for the composites prepared with different amount of Ag$^+$, and Ag^0 elution did not change the specific surface area of TiO$_2$.

3.2. The chemical nature of Ag element in the catalysts

The chemical nature of Ag element in the catalysts was further investigated with XPS spectra. The XPS survey spectra shows that the determined Ag content in 2% Ag-loaded TiO$_2$ composites decreased from 0.25% to only 0.03% after the K$_3$[Fe(CN)$_6$]/aqueous ammonia eluting, which confirmed that most of Ag was eluted from the composite. Meanwhile, post-adsorption of Ag$^+$ cation increased the Ag content from 0.03% to 0.10%, which indicated some Ag$^+$ cation was chemically adsorbed onto the surface of TiO$_2$. Fig. 4 presents the Ag$_{3d}$ fine XPS spectra of 2% Ag^0/Ag$^+$/TiO$_2$, 2% Ag$^+$/TiO$_2$ and 2% P-Ag$^+$/TiO$_2$. Ag$^0_{3d}$ atom has binding energies of 367.3 eV and 373.2 eV, which can be obviously observed in the Ag$_{3d}$ fine XPS spectra of 2% Ag^0/Ag$^+$/TiO$_2$. The XPS signals of 2% P-Ag$^+$/TiO$_2$ could be dominantly ascribed to the TiO$_2$ surface adsorbed Ag$^+_{3d}$, which have a slight shift (+0.3 eV) and give binding energies of 367.6 eV and 373.5 eV. Interestingly, the XPS spectrum of 2% Ag$^+$/TiO$_2$ gives four signals at 367.6 eV, 370.4 eV, 373.5 eV and 376.3 eV. Besides the signals from the surface adsorbed Ag$^+_{3d}$, two additional signals at 370.4 eV and 376.3 eV could be due to another form of Ag species that differs from Ag^0 atom in Ag^0 clusters and surface adsorbed Ag$^+$ cation. The amount of this special Ag species is very limited and its signals are generally overwhelmed with that of Ag^0 (in 2% Ag^0/Ag$^+$/TiO$_2$) and Ag$^+$ (in 2% P-Ag$^+$/TiO$_2$). As it is resistant to the K$_3$[Fe(CN)$_6$]/aqueous ammonia eluting, we deem it should be a kind of Ag$^+$ which has strong chemical bonds with the oxygen atoms. Predictably, it should be Ag$^+$ cation that just fills in the interfacial lattice defect sites of TiO$_2$ and thus chemically coordinated with oxygen atoms to form O^{2-}—Ag$^+$—O^{2-} joint.
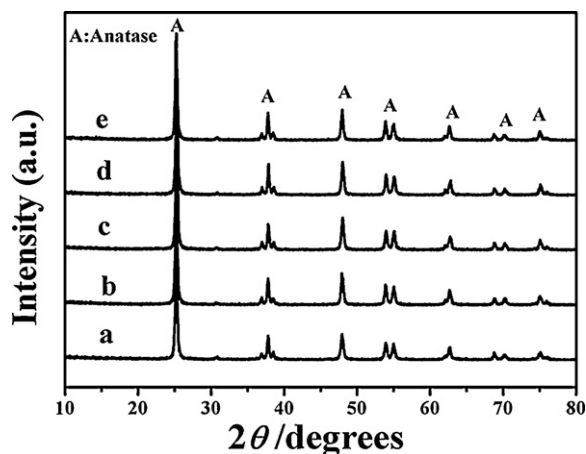

Fig. 2. XRD patterns of the (a) 0.0%, (b) 1%, (c) 2%, (d) 3%, and (e) 4% Ag-loaded TiO$_2$ after the K$_3$[Fe(CN)$_6$]/aqueous ammonia elution.
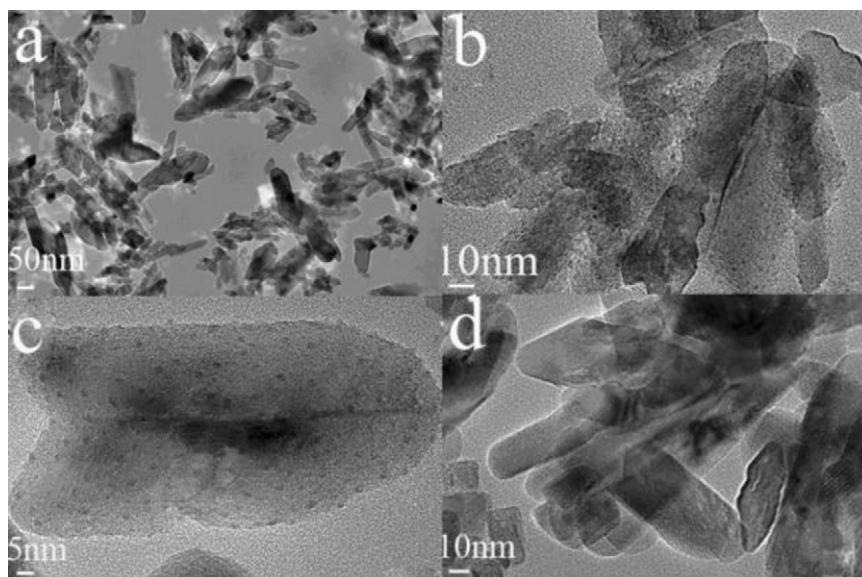
Fig. 3. (a–c) HRTEM images of 2.0% $Ag^0/Ag^+/TiO_2$ and (d) 2.0% Ag^+/TiO_2.

Fig. 4. Ag_{3d} XPS spectra of (a) 2% $Ag^0/Ag^+/TiO_2$, (b) 2% Ag^+/TiO_2, and (c) 2% P-Ag^+/TiO_2.

3.3. Photocatalytic performance of catalysts

The photocatalytic performance of above Ag modified titania composites were investigated with the degradation of two frequently used model pollutants, MO ($10 \, mg \, L^{-1}$) and RhB ($20 \, mg \, L^{-1}$) under UV irradiation. As usual, the deposition of Ag^0 clusters enhances the photocatalytic activity of the photocatalyst at low amount and then is adverse at higher dosages (Fig. 5a). 1% $Ag^0/Ag^+/TiO_2$ provides the highest photocatalytic activity among all $Ag^0/Ag^+/TiO_2$ composites and gives a MO photocatalytic degradation rate of 59.5% in 2 h, while that of the bare TiO_2 is 56%. In a word, the depositions of Ag^0 clusters do not improve much the photocatalytic performance of TiO_2. After the K_3 [Fe (CN) $_6$]/aqueous ammonia eluting, the photocatalytic activity of the corresponding photocatalysts enhanced a lot (Fig. 5). As for the 1% series composites, 1% Ag^+/TiO_2 gives a MO degradation rate of 77.7% in 2 h, which is increased by ca. 20% to that of 1% $Ag^0/Ag^+/TiO_2$. More significantly, the MO degradation rates of 2%, 3% and 4% Ag^+/TiO_2 also present values of 78.6%, 79% and 75%, respectively, which have increments of 30.6%, 35%, and 40% to their corresponding $Ag^0/Ag^+/TiO_2$ composites, respectively. Notably, the photocatalytic

Table 1

Physical properties of Ag surface modified titania. Numbers in sample names represent $AgNO_3$/TBT mole ratio in the hydrothermal preparation. ND: not detectable.

Sample	Specific surface area (m²/g)[a]	Surface metal content (atm%)[b]	Crystallite size (nm)	
			TiO_2[c]	Ag^0[d]
1.0% $Ag^0/Ag^+/TiO_2$	34.77	0.16	38.0	~2.2
1.0% Ag^+/TiO_2	32.48	0.01	37.5	ND
1.0% P-Ag^+/TiO_2	34.2	0.08	37.4	ND
2.0% $Ag^0/Ag^+/TiO_2$	34.7	0.25	39.2	~2
2.0% Ag^+/TiO_2	31.5	0.03	39.1	ND
2.0% P-Ag^+/TiO_2	30.7	0.10	38.5	ND
3.0% $Ag^0/Ag^+/TiO_2$	32.49	0.26	38.3	~1.5
3.0% Ag^+/TiO_2	32.45	0.02	38.3	ND
3.0% P-Ag^+/TiO_2	31.13	0.08	38.1	ND
4.0% $Ag^0/Ag^+/TiO_2$	29.17	0.35	39.2	~2
4.0% Ag^+/TiO_2	30.42	0.02	38.8	ND
4.0% P-Ag^+/TiO_2	29.11	0.09	39.1	ND

[a] Specific surface area was measured with N_2 adsorption–desorption isotherm.

[b] Surface metal content was determined by XPS.

[c] Crystallite size of TiO_2 was determined by XRD with the Scherrer equation.

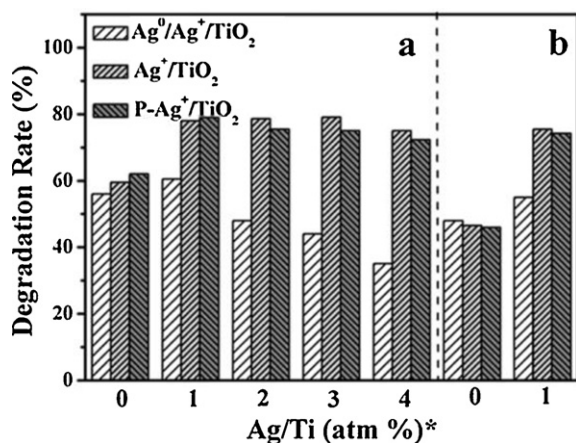[d] Crystallite size of Ag^0 was measured by HRTEM.

Fig. 5. UV photocatalytic degradation rates of (a) MO ($10 \, mg \, L^{-1}$) and (b) RhB ($20 \, mg \, L^{-1}$) with various Ag modified TiO_2 composites in 2 h. Photocatalyst dosage: $10 \, mg \, L^{-1}$; light source: 300 W high pressure Hg lamp [16] (*$AgNO_3$/TBT mole ratio in the hydrothermal preparation (%)).

Fig. 6. UV photocatalytic degradation of MO ($10 \, mg \, L^{-1}$) with bare TiO_2 and various Ag modified TiO_2 composites. 0.12 M and 0.25 M refer to the total concentrations of $NaNO_3 + AgNO_3$.

activity of all the Ag^+/TiO_2 composites is maintained at high levels ($77\% \pm 2\%$) with very slightly changes. Considering that the photocatalytic activity of bare TiO_2 (i.e. 0% series) keeps almost unchanged after the $K_3[Fe(CN)_6]$/aqueous ammonia eluting with a MO degradation rate of 59.6%, the effective constituents which activate the Ag^+/TiO_2 composites are apparently retained or even enhanced after the removal of Ag^0 clusters. It is thus readily to get a conclusion that the left Ag^+ cations make the main contribution to promote the photocatalytic activity of the com-
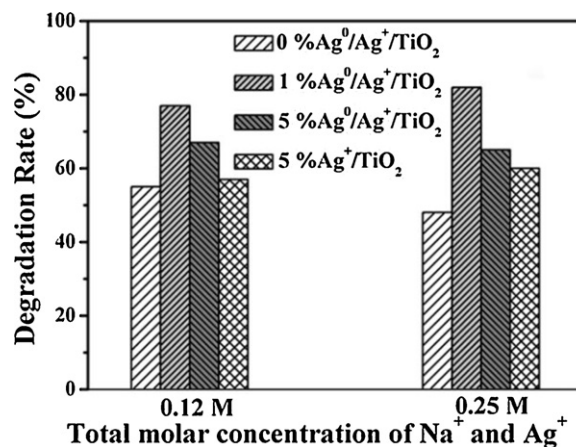
posites, and the removal of Ag^0 clusters would expose additional interfacial Ag^+ cations which previously covered with the Ag^0 clusters. The amount of surface adsorption of Ag^+ cations can be further improved with post-adsorption operation. However, $P-Ag^+/TiO_2$ only gives MO degradation rates of 62%, 80%, 75.5%, 75% and 72.3% for bare TiO_2, P-1% Ag/TiO_2, P-2% Ag/TiO_2, P-3% Ag/TiO_2 and P-4% Ag/TiO_2, respectively, which change little from their corresponding Ag^+/TiO_2 composites and thus deny a significant promotion role of chemical adsorbed Ag^+ cations. The photocatalytic degradation
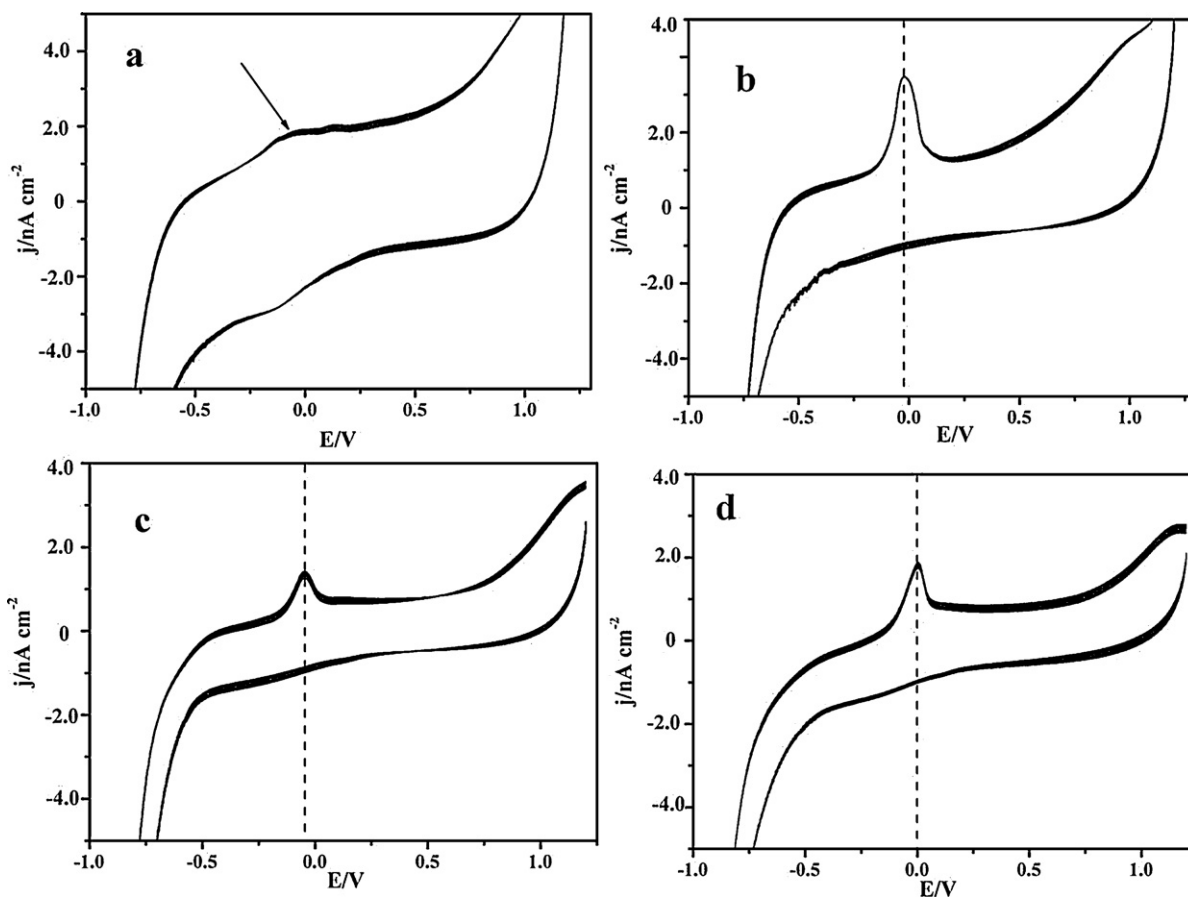

Fig. 7. CV curves of (a) TiO_2; (b) $Ag_m^0 \rightarrow Ag_m^+$; (c) $Ag_n^0 \rightarrow Ag_n^+$ in $Ag^0/Ag^+/TiO_2$ and (d) $O^{2-}-Ag^0-O^{2-} \rightarrow O^{2-}-Ag^+-O^{2-}$ in Ag^+/TiO_2. *Ag_m^0 is Ag^0 nanoparticles in situ prepared on the SPCE electrode by electrodeposition from $AgNO_3$ aqueous solution.

of RhB (Fig. 5b) gives just similar results, that is, elution-resistant Ag^+ cations, but neither Ag^0 clusters nor chemical adsorbed Ag^+ cations, should be responsible for the photocatalytic performance improvement of the Ag modified titania in this work.

It is worth mentioning that if Ag-loaded TiO_2 in this work is prepared with the just same procedure but in the presence of sodium salt (which is a very promising method for preparing brookite TiO_2 [17]), the $K_3[Fe(CN)_6]$/aqueous ammonia eluting regrettably harms to the photocatalytic activity of the composites. As shown in Fig. 6, although the photocatalytic activity of each eluted composite is slightly higher than that of its corresponding bare TiO_2, it is definitely lower than that of Ag^0 cluster loaded TiO_2.

A most probable reason is that the interfacial lattice defect sites in this case are predominantly occupied by Na^+ cation, as Na^+ cation has a stronger electrostatic interaction with $[TiO_6]$ octahedral. Therefore, the presence of Na^+ ion during the hydrothermal preparation of $Ag^0/Ag^+/TiO_2$ is adverse to the formation of interfacial lattice Ag^+ ion. The doping of Ag^+ ion is mostly diminished and the promotion effect of Ag^+ ion is obliterated by Na^+ cation.

3.4. Mechanism explanation for enhanced photocatalytic reactivity of the catalysts

The photocatalytic performance of a photocatalyst relates closely to its photogenerated charge carriers behaviors. Thus, the redox potentials of the Ag species in $Ag^0/Ag^+/TiO_2$ and Ag^+/TiO_2 composites were observed with CV method.

Fig. 7 shows the CV curves of TiO_2, $Ag^0/Ag^+/TiO_2$, Ag^+/TiO_2 and reference Ag^0 nanoparticles. Although the reduction peaks may not be visible in the cathodic sweep, the oxidation peak of TiO_2 on the CV scan can be observed at ca. -0.07 V (Fig. 7a) and the oxidation peaks of Ag^0 clusters ($Ag_n^0 \to Ag_n^+$) in $Ag^0/Ag^+/TiO_2$ and doped Ag^+ ($O^{2-}-Ag^0-O^{2-} \to O^{2-}-Ag^+-O^{2-}$) in Ag^+/TiO_2 are presented at ca. -0.05 V (Fig. 7c) and 0.00 V (Fig. 7d), respectively. As a reference, the oxidation peak of Ag^0 nanoparticles in situ prepared with electrodeposition method on the SPCE electrode ($Ag_m^0 \to Ag_m^+$) appears at ca. -0.02 V in Fig. 7b. The CV results show that the redox potential of doped Ag^+ is relatively more positive than those of TiO_2 and Ag^0 clusters. Thus, it is really possible that the surface lattice doped Ag^+ would capture the photogenerated electrons and benefits the photocatalytic activity of composites by promoting the separation of photogenerated electrons and holes.

Presumably, the $O^{2-}-Ag^+-O^{2-}$ joint at the interfacial lattice defect sites of TiO_2 is the key for the superior photocatalytic activity of Ag^+/TiO_2. Supposedly, the $O^{2-}-Ag^+-O^{2-}$ would intervene into and improve the kinetic processes of the photogenerated carriers. The photogenerated electrons would be captured with the $O^{2-}-Ag^+-O^{2-}$ joint to form $O^{2-}-Ag^0-O^{2-}$, which is however instable and prefer to react with surface adsorbed oxygen molecules, that is electron acceptor. In this way, interfacial lattice Ag^+ cations work as perfect electron medium to achieve a better separation of photogenerated electrons and holes as well as catalyze the reaction of electron with O_2. The most attractive is the fact that the as-formed interfacial lattice Ag^+ cations are recyclable during the whole process, while those surface chemical adsorbed Ag^+ cations are of one-time consumption [20,21]. The turn over number of the interfacial lattice Ag^+ cations in Ag^+/TiO_2 can be over 8 MO (and 10 RhB) per Ag^+ cation in 2 h even roughly regarding the XPS measured Ag content as total Ag^+ content in the composite (in general, the XPS measured Ag content is much higher than the nominal total Ag^+ content in Ag modified TiO_2).

4. Conclusions

$Ag^0/Ag^+/TiO_2$ composites was prepared via an alkalescent hydrothermal process, and Ag^+/TiO_2 was prepared by eluting the Ag^0 cluster from the $Ag^0/Ag^+/TiO_2$ composites with $K_3[Fe(CN)_6]$/aqueous ammonia. The photocatalytic activity of the composites were greatly enhanced after eluting the Ag^0 cluster from the $Ag^0/Ag^+/TiO_2$ composites, which suggests that interfacial lattice Ag^+ cations play a dominant role in the photogenerated charge carriers separation in the Ag modified titania prepared in this work. Further, the presence of Na^+ cation during the hydrothermal preparation of $Ag^0/Ag^+/TiO_2$ is adverse and surface chemical adsorbed Ag^+ cation is invalid to the promotion effect of interfacial lattice Ag^+ cations, which suggest the chemical state is essential to the promotional effect of the interfacial lattice Ag^+ cation. The 2 h turn over number of the interfacial lattice Ag^+ cations to the degradation of MO and RhB shows that the interfacial lattice Ag^+ cations act as recyclable catalytic sites but not one-time consumptive species.

References

[1] M.R. Hoffmann, S.T. Martin, W. Choi, D.W. Bahnemann, Chemical Reviews 95 (1995) 69–96.
[2] T.L. Thompson, J.T. Yates, Chemical Reviews 106 (2006) 4428–4453.
[3] T. Hirakawa, P.V. Kamat, Journal of the American Chemical Society 127 (2005) 3928–3934.
[4] R. Abe, H. Takami, N. Murakami, B. Ohtani, Journal of the American Chemical Society 130 (2008) 7780–7781.
[5] W.T. Sun, Y. Yu, H.Y. Pan, X.F. Gao, Q. Chen, L.M. Peng, Journal of the American Chemical Society 130 (2008) 1124–1125.
[6] H. Choi, R. Nicolaescu, S. Paek, J. Ko, P.V. Kamat, ACS Nano 5 (2011) 9238–9245.
[7] I.V. Lightcap, T.H. Kosel, P.V. Kamat, Nano Letters 10 (2010) 577–583.
[8] H. Zhang, X.J. Lv, Y.M. Li, Y. Wang, J.H. Li, ACS Nano 4 (2010) 380–386.
[9] V. Subramanian, E.E. Wolf, P.V. Kamat, Journal of the American Chemical Society 126 (2004) 4943–4950.
[10] C.G. Silva, R. Juárez, T. Marino, R. Molinari, H. García, Journal of the American Chemical Society 133 (2011) 595–602.
[11] X. Chen, H.Y. Zhu, J.C. Zhao, Z.F. Zheng, X.P. Gao, Angewandte Chemie International Edition 47 (2008) 5353–5356.
[12] K. Awazu, M. Fujimaki, C. Rockstuhl, J.J. Tominaga, H. Murakami, Y. Ohki, N. Yoshida, T. Watanabe, Journal of the American Chemical Society 130 (2008) 1676–1680.
[13] H.G. Boyen, G. Kästle, F. Weigl, B. Koslowski, C. Dietrich, P. Ziemann, J.P. Spatz, S. Riethmüller, C. Hartmann, M. Möller, G. Schmid, M.G. Garnier, P. Oelhafen, Science 297 (2002) 1533–1536.
[14] J.X. Li, J.H. Xu, W.L. Dai, K.N. Fan, Journal of Physical Chemistry C 113 (2009) 8343–8349.
[15] Q. Fu, H. Saltsburg, M. Flytzani-Stephanopoulos, Science 301 (2003) 935–938.
[16] B. Zhao, F. Chen, Y.C. Jiao, H.Y. Yang, J.L. Zhang, Journal of Molecular Catalysis A: Chemical 348 (2011) 114–119.
[17] B. Zhao, F. Chen, Y.C. Jiao, J.L. Zhang, Journal of Materials Chemistry 20 (2010) 7990–7997.
[18] Y.C. Jiao, B. Zhao, F. Chen, J.L. Zhang, CrystEngComm 13 (2011) 4167–4173.
[19] B. Zhao, F. Chen, Q.W. Huang, J.L. Zhang, Chemical Communications 34 (2009) 5115–5117.
[20] L.B. Yang, X. Jiang, W.D. Ruan, J.X. Yang, B. Zhao, W.Q. Xu, J.R. Lombardi, Journal of Physical Chemistry C 113 (2009) 16226–16231.
[21] K. Naoi, Y. Ohko, T. Tatsuma, Journal of the American Chemical Society 126 (2004) 3664–3668.